The International Journal of
Robotics Research
0(0) 1–11

DOI: 10.1177/0278364912455073
ijr.sagepub.com

Progress on 'pico' air vehicles

RJ Wood[1,2], B Finio[1,2], M Karpelson[1,2], K Ma[1,2], NO Pérez-Arancibia[1,2], PS Sreetharan[1,2], H Tanaka[1,2] and JP Whitney[1,2]

Abstract

As the characteristic size of a flying robot decreases, the challenges for successful flight revert to basic questions of fabrication, actuation, fluid mechanics, stabilization, and power, whereas such questions have in general been answered for larger aircraft. When developing a flying robot on the scale of a common housefly, all hardware must be developed from scratch as there is nothing 'off-the-shelf' which can be used for mechanisms, sensors, or computation that would satisfy the extreme mass and power limitations. This technology void also applies to techniques available for fabrication and assembly of the aeromechanical components: the scale and complexity of the mechanical features requires new ways to design and prototype at scales between macro and microeletromechanical systems, but with rich topologies and material choices one would expect when designing human-scale vehicles. With these challenges in mind, we present progress in the essential technologies for insect-scale robots, or 'pico' air vehicles.

Keywords

microrobots, micro air vehicles, aerial robotics

1. Introduction

Over the past several decades there have been multiple research projects aimed at the development of a flapping-wing robotic insect. These include a butterfly-like ornithopter from the University of Tokyo (Tanaka et al., 2005), the 'Micromechanical Flying Insect' project at U.C. Berkeley (Fearing et al., 2000, 2002), and the Harvard 'RoboBee' project (Wood, 2008). These efforts are motivated by tasks such as hazardous environment exploration, search and rescue, and assisted agriculture, similar to the tasks cited for many autonomous robots regardless of scale or morphology. Using swarms of small, agile, and potentially disposable robots for these applications could have benefits over larger, more complex individual robots with respect to coverage and robustness to robot failure. But the interest in these types of robots goes well beyond the expected tasks; use as tools to study open scientific questions (e.g. fluid mechanics of flapping flight, control strategies for computation and sensor-limited systems) and the necessary technological achievements that must accompany these projects are the real motivations.

Work in unmanned aerial vehicles has a rich history that spans from scientific inquiry to congressional policy.[1] In 1997, the United States Defense Advanced Research Projects Agency (DARPA) announced its 'Micro Air Vehicle' (MAV) program which defined a MAV as being 15 cm or less in largest linear dimension, have a range of 10 km, peak velocities over 13 m/s, and operate for more than 20 minutes.[2] Performers in this program developed multiple successful MAV prototypes including the Black Widow and Microbat (Keennon and Grasmeyer, 2003) as well as some of the first examples of piezoelectric-actuated MAVs (Cox et al., 2002; Fearing et al., 2000). In 2005, DARPA again pushed the limits of aerial robotics by announcing the 'Nano Air Vehicle' program,[3] which had the requirements of 10 g or less vehicles with 7.5 cm maximum dimension, able to fly 1 km or more. Results include the 16cm, 19g 'Nano Hummingbird' from Aerovironment,[4] the maple seed-inspired Lockheed 'Samarai'[5], and a coaxial

[1]School of Engineering and Applied Sciences, Harvard University, Cambridge, MA, USA
[2]Wyss Institute for Biologically Inspired Engineering, Cambridge, MA, USA

Corresponding author:
RJ Wood, Harvard School of Engineering and Applied Sciences, 33 Oxford Street, Cambridge, MA 02138.
Email: rjwood@seas.harvard.edu

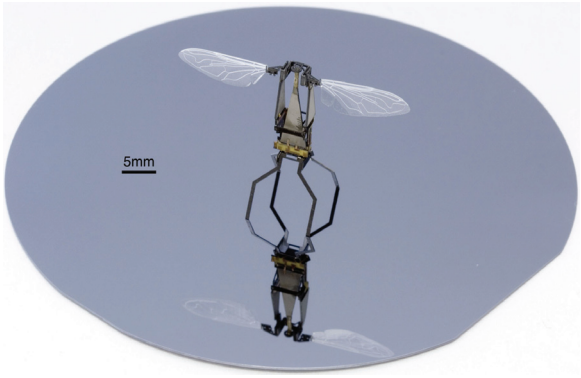

Fig. 1. Example of a recent prototype of a 'RoboBee'. These two-wing, 100 mg robots are capable of controlled thrust and body moments.

helicopter from a Draper Labs led team.[6]. There are also a number of recent commercially available flapping-wing toy ornithopters and RC helicopters on the scale of MAVs such as the Silverlit 'iBird' and the Wowwee Flytech toys.[7]

Using these trends, we define a 'pico' air vehicle as having a maximum takeoff mass of 500 mg or less and maximum dimension of 5 cm or less. This is in the range of most flying insects (Dudley, 1999), and thus for pico air vehicles we look primarily to insects for inspiration. An example prototype pico air vehicle, a prototype from the Harvard RoboBee project,[8] is shown in Figure 1. This paper presents an overview of progress on component technologies for a pico air vehicle. Each one of these topics is the subject of significant research (highlighted where appropriate in this article) and as such this paper is not intended to describe any of these topics in great depth. Furthermore, we only discuss flapping-wing propulsion. The rationale for this choice is based on two scaling considerations. First, as the characteristic length of a vehicle is reduced (e.g. mean chord length), the lift-to-drag ratio will generally decrease for fixed and rotary wing aircraft. Second, fixed and rotary wing aircraft typically rely on continuously rotating components to generate propulsion for flight. As will be discussed later, rotating mechanisms (e.g. bearings, gears, motors) become problematic to manufacture at small scales and may experience significantly reduced performance compared to more macro-scale counterparts.

Regardless of the classification, the challenges of creating effective flying robots span many disciplines. For example, fluid mechanics changes as a function of characteristic length and velocity: MAVs on the scale of large birds (Re $>$ 10,000) exist in a regime of turbulent flow and steady lift to drag ratios greater than 10 (Dudley, 1999). Nano air vehicles may exist in the transition region (1000 $<$ Re $<$ 10,000) and thus the impact of boundary layer separation (and potential reattachment) becomes particularly relevant. Whereas for pico air vehicles (Re $<$ 3000), the flow is almost entirely laminar and thus so-called 'unsteady' mechanisms can be employed to enhance lift beyond what would be achievable from constant velocity alone. Nonetheless, it appears that the energetic cost for flight in artificial systems, when considering a metric similar to cost of transport, increases with decreasing characteristic length. Where we could expect a larger-scale aircraft (tens of meters in characteristic dimension) to stay aloft for many hours or even days, flight times for micro, nano, and pico air vehicles are expected to be of the order of an hour, a few tens of minutes, and less than 10 minutes, respectively (Karpelson et al., 2010).

Similar scaling trends also exist for device manufacturing. It is useful to make a distinction between 'feature size' and 'characteristic size' as pertaining to a vehicle: the former refers to the smallest dimension of the mechanical components of the system, the pitch of gear teeth, thickness of a constituent material, and length of a flexure are examples, while the latter is more descriptive of the overall scale of the vehicle and can refer to the wingspan, chord length, or some similar quantity. We make the argument that as the characteristic size of a vehicle is reduced, feasible approaches to fabrication and assembly of the various propulsion and control mechanisms makes a distinct transition between more standard approaches using 'off-the-shelf' components and machining and assembly tools to requiring entirely novel methods. This is one of the fundamental challenges for creating a pico air vehicle. Successful attempts at reducing the scale of terrestrial (Brooks and Flynn, 1989; Caprari et al., 2002) and aerial (Lentink et al., 2009) robots illustrate these challenges. As the feature sizes of the mechanical components are decreased below around 10–100 μm, the designer can no longer rely on standard macro-scale machining techniques. Even high-resolution CNC mills,[9] with positioning accuracy down to 1 μm, require end mills that are rare or non-existent below 50–100 μm. Furthermore, the physics of scaling dictates that as the feature size is decreased, area-dependent forces (e.g. friction, electrostatic, and van der Waals) become dominant, causing more traditional bearing joints to be very lossy with respect to power transmission (Trimmer, 1989). Similar arguments can be made for transducers. As the feature size is reduced, friction losses and limits on current density decrease the effectiveness of electromagnetic motors (Trimmer, 1989). For example, the induction motor in a Tesla Roadster can produce over 7 kW/kg at nearly 90% transduction efficiency[10] whereas the smallest DC motors commercially available can produce 39 W/kg at less than 18% efficiency.[11,12] A deeper discussion of actuator geometries and materials will be presented in Section 2.2. Regardless of the transduction mechanism, it is clear that a pico air vehicle will require non-traditional solutions to device fabrication. MEMS (microelectromechanical systems) surface micro-machining techniques offer one path to achieve micrometer-order feature sizes. However, these techniques are hindered by the time-consuming serial nature of the process steps, limited three dimensional capabilities, and the high cost of prototyping using MEMS foundries. A solution for fabrication and assembly of a pico air vehicle will

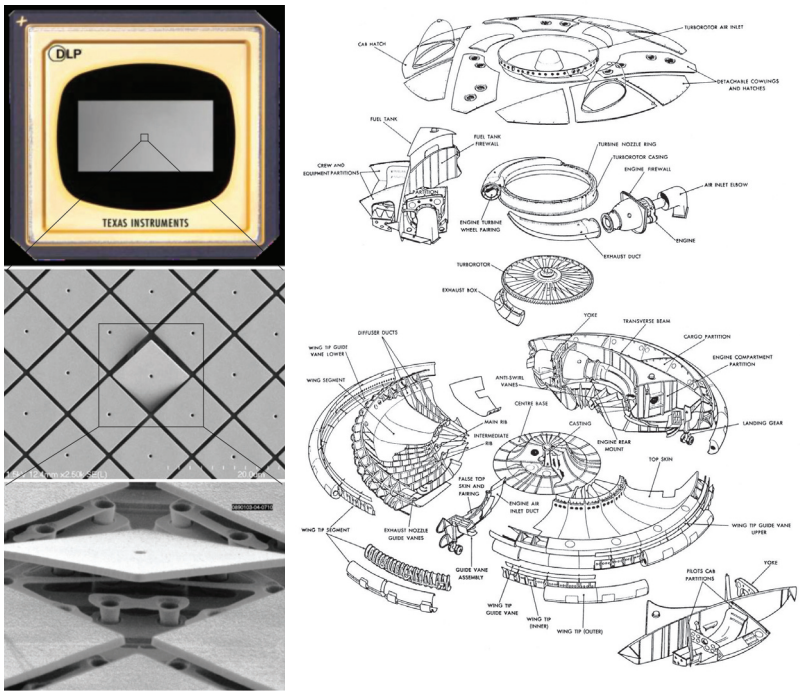

Fig. 2. At two ends of the fabrication and assembly spectrum: MEMS surface micromachined mirrors from a Texas Instruments DLP display (left, images courtesy of Jack Grimmet and Martin Izzard, Texas Instruments) and a 'nuts-and-bolts' approach to assembly of a complex macro-scale device: an experimental 'human-scale' hover-capable aircraft, the 'Avrocar' (Avro Canada, 2010) (right).

be described in Section 2.4 and examples of both ends of the fabrication spectrum are shown in Figure 2.

Challenges for control are also scale-dependent. Larger-scale vehicles can take advantage of passive stability mechanisms (e.g. positive wing dihedral) and generally have larger mass and power capacity for various sensors and computer architectures. An insect-scale device will have significantly reduced payload capacity as compared with a micro or even nano air vehicle. Therefore, the control challenges for a pico air vehicle are currently centered around flight stabilization using limited sensing and computation capabilities. This is in contrast to 'higher-level' control problems of autonomous navigation (Shen et al., 2011) and coordination of multiple unmanned air vehicles (Stirling and Floreano, 2010).

Beyond aeromechanics, actuation, fabrication, and control, there are numerous additional issues including power, system-level design, integration, and mass production. Thus, the challenges for a pico air vehicle are daunting, yet form a set of exciting and well-posed engineering questions and scientific opportunities. The remainder of this article will discuss recent progress in a number of these areas.

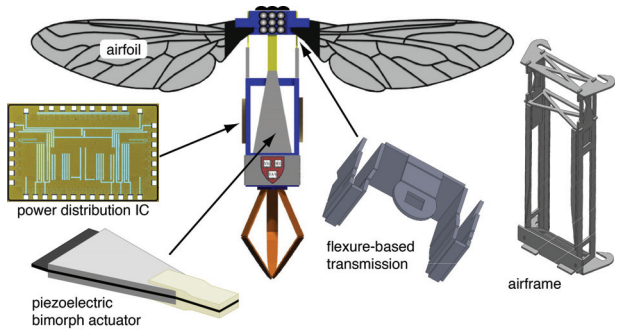

Fig. 3. Components of a pico air vehicle.

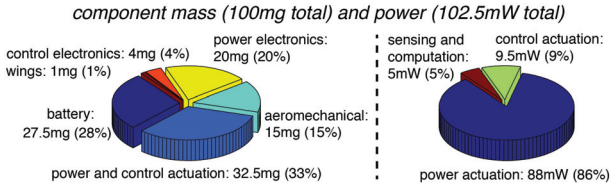

Fig. 4. Mass (left) and power (right) budgets for a 100 mg robot, derived using the method in Karpelson et al. (2010).

2. Overview of a pico air vehicle

This article will focus on some of the key components of a flapping-wing pico air vehicle, as shown in Figure 3, based on the design of the Harvard RoboBee. These components make up the majority of the power and mass budget for the pico air vehicle, which is shown in Figure 4 for a hypothetical 100 mg robot. Note the dominance of battery and actuator mass and actuator power, which is indicative of the energetic cost of flight at these scales.

Fig. 5. Illustration of one-half cycle of wing motion (i.e. the down stroke) for a Diptera assuming negligible stroke plane deviation. Top row: lateral perspective. Bottom row: dorsal perspective.

2.1. Aeromechanics

Owing to the scaling of fluid properties, insects operate in a fundamentally different way than conventional aircraft. Although there are many, sometimes subtle, differences between the flight apparatuses of individual species, in general, insects have one or two pairs of wings, driven in multiple rotational degrees of freedom (DOFs) by flight musculature, and powered by metabolic processes which convert chemical energy for flight. For a flapping-wing pico air vehicle, we derive some design principles from Dipteran (two-winged) insects. We assume that each wing has two rotational DOFs: flapping and rotation about an axis approximately parallel to the leading edge (i.e. pronation and supination). During flapping, the upstroke and downstroke are assumed to be nominally symmetric with no stroke plane deviation. The wing motion is illustrated in Figure 5. Thinking about the propulsion mechanism as a lumped-parameter second-order system, the dominant components are the inertia of the wing, potential energy storage in the muscles, plates, and joints of the thorax, and the damping due to interaction between the wing and the air. As with Diptera and other insects which use 'indirect' flight muscles, we assume that the wing drive for a flapping-wing pico air vehicle will also operate at resonance to amplify the wing stroke (Dudley, 1999).

In order to control motion in these two DOFs, the actuators are coupled to the wings using a flexure-based articulated transmission mechanism (see Figure 3). Previous designs utilized a spherical five-bar mechanism to map two linear actuator inputs to the two wing DOFs (Avadhanula et al., 2002). Kinematically, this allows direct control over the phasing of wing rotation and any asymmetries in between the upstroke and downstroke. However, dynamic coupling between the two DOFs creates challenges for controlled trajectories at the flapping resonant frequency. Instead, an under-actuated version of the transmission includes a passive flexure hinge at the wing base such that flapping is commanded by a single power actuator and rotation is passive (Wood, 2007). Tuning the dynamics of the system at design time places the rotational resonance well above the flapping resonance such that we can assume quasi-static wing rotation while driving the actuator at the first flapping resonant frequency. There is evidence that wing rotation in some insects is driven by inertial and aerodynamic forces, as opposed to directly activated by thoracic musculature (Ennos, 1988b,a; Bergou et al., 2007).

The presence of unsteady flow features arising from wing–wake and wing–wing interactions, aeroelastic coupling between fluid pressure and wing bending (Combes and Daniel, 2003a,b), and the significance of vortex formation and shedding (Dickinson et al., 1999) result in challenges for a succinct description of the relationship between wing properties (geometric, inertial, and elastic), wing motions and deformation, and resulting flow and force generation. To study the aeromechanics of flapping-wing flight, researchers have employed a variety of methods including dynamic scaling (Dickinson et al., 1999), computational fluid dynamics (CFD) methods (Mittal and Iaccarino, 2005), and direct biological observation (Ellington et al., 1996). Each of these has led to significant insights into the details of flow structure, performance of many flying insects, and the function of various morphological features. A combination of these methods, the 'blade-element' method (Whitney and Wood, 2010), merges quasi-steady flow analysis with empirically fit force and torque coefficients which hide all of the unsteady terms behind these coefficients. This has allowed designers to study a variety of wing morphologies and trajectories. In some cases, the aeroelastic interaction between strain energy in the airfoil and fluid pressure may have a non-negligible effect on the dynamics and energetics of the vehicle. In such cases, it is valuable to study the fluid mechanics using either a coupled fluid–structure CFD code or at-scale experiments which do not make any scaling assumptions on wing compliance. Furthermore, inertial effects cannot be commensurately scaled in dynamically scaled models. Dynamically scaled models which use water, mineral oil, or a similar fluid will have absolute densities of the order of 1,000 kg/m^3, roughly three orders of magnitude greater than air. In order to match the inertial effects relative to the inertia of the wing would require a wing material three orders of magnitude more dense than insect cuticle (1–1.3 $\times$ 10^6 g/m^3 (Vincent and West, 2004)), requiring a density of approximately 1 $\times$ 10^9 g/m^3. Even if the wing were allometrically scaled in such a way that the thickness were increased by a factor of 10 relative to the isometrically scaled geometry, this would still require a density of 1 $\times$ 10^8 g/m^3, approximately 50 times greater than osmium (density of 22.6 $\times$ 10^6 g/m^3). This is often a benefit for dynamically scaled models; if inertial forces are negligible, measured forces are predominantly from fluid interactions.

Given the ability to manufacture insect-scale airfoils, such as the *Eristalis* wing in Figure 6 (Tanaka and Wood, 2010), and actuate them with insect-like trajectories and wingbeat frequencies, we have begun multiple experiments which are aimed at a deeper understanding of the fluid mechanics for a pico air vehicle with emphasis on learning design rules to enhance aerodynamic efficiency and, thus,

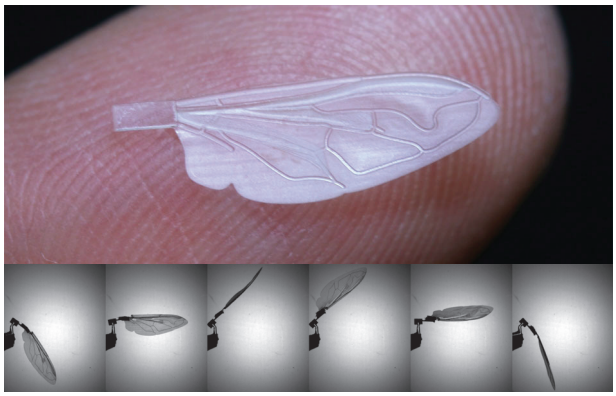

Fig. 6. Photo of a micromolded polymer wing mimicking the features of an *Eristalis* wing (top). This wing was created in a single molding step and includes veins ranging from 50–125 μm thick, 100 μm corrugation, and a 10–20 μm membrane. A sample of the wing motion (dorsal perspective) at 150 Hz flapping frequency taken from a high-speed video (bottom).

the overall performance of the robot. Recent experiments include the following:

- The development of multiple methods to create biomimetic airfoils and verification that the static characteristics are consistent with biological wings (Shang et al., 2009; Tanaka and Wood, 2010).
- The establishment of a blade-element-based model of under-actuated flapping dynamics (i.e. passive rotation) and validated using a custom-made single flapping-wing, high-resolution force sensing (Wood et al., 2009), and high-speed motion reconstruction (Whitney and Wood, 2010).
- Exploration of the function of distributed versus localized wing compliance on lift force generation (Tanaka et al., 2011).

2.2. Actuation

As discussed previously, the physics of scaling requires us to seek an alternative to electromagnetic actuation for a pico air vehicle. But there are more subtle reasons for this as well. Even if the power densities and efficiencies were comparable, the unloaded RPM of a rotary electromagnetic motor will typically increase with decreasing size, thus requiring substantial gearing to produce useful work and increasing the overall complexity of the transmission system. Furthermore, as we are assuming a reciprocating flapping motion, a rotary motor would require additional transmission components (and rotary bearings) to convert the rotation to wing flapping, again increasing part count and complexity. Instead we look to oscillatory actuators and in particular induced-strain materials. Induced-strain materials respond to an applied stimulus with a simple change in geometry. There are multiple options including piezoelectric, electroactive polymers, solid-state phase transitions, electrostriction, and thermal expansion. There have also been many demonstrations of relatively simple geometries for producing linear actuation from electrostatic forces (Tang et al., 1990), clever piezoelectric linear motors,[13] piezoelectric stacks and 'moonie'-type actuators (Newnham et al., 1993), and many dielectric elastomer configurations (Pelrine et al., 2001). Other types of oscillatory actuators can be created without induced-strain materials, for example using electrostatic or electromagnetic forces. Electrostatic actuators are common in MEMS applications (Bellew et al., 2003); however, they bring challenges in scaling up to millimeter-scale devices. Electromagnetic linear actuators (e.g. solenoids and voice coils) are common for macro-scale applications, however the scaling of magnetic forces reduces the effectiveness for microrobots.[14]

Each material and actuator morphology can be evaluated based on the standard metrics of blocked force, free displacement (and thus energy), density (and thus energy density), bandwidth (and thus power density), and efficiency. However, the focus is not only on performance, but also practicality. Therefore, additional considerations include fabrication complexity, cost, robustness, the drive method, and linearity of the input–output response and any related control issues. Figure 7 qualifies actuation options relative to some of these metrics. Note that other qualitative actuator metrics can be inferred from this figure. For example, maximum power can be inferred from the product of maximum stress and maximum strain (i.e. mechanical work) and bandwidth. Power density can be inferred from the maximum power and the density metric in Figure 7. Power source size can be inferred from the power and efficiency metrics. A more comprehensive and quantitative study of actuation choices for a pico air vehicle, along with associated power electronics options, is presented in Karpelson et al. (2008) with reference to multiple flapping-wing design break points.

Given the needs of a pico air vehicle, we chose clamped–free bending bimorph polycrystalline piezoelectric actuators as a local minimum in complexity while meeting the key specifications for bandwidth, power density, and efficiency. Furthermore, we can rapidly prototype many geometries and obtain all necessary materials commercially. Note that the use of these piezoelectric actuators also carries some important scaling decisions since we are assuming a resonant primary drive. Considering only structural scaling, the resonant frequency will monotonically increase with decreasing size[15] (this trend can be seen clearly in insects (Dudley, 1999)). For quasi-static operation of piezoelectric actuators, power density will increase roughly linearly with operating frequency. Thus, for smaller devices, this type of actuator is attractive and can out perform insect flight muscle by a factor of two or more in power density (Steltz and Fearing, 2007). The opposite trend is true as well: it is clear that, for direct-drive transmissions, above a certain size these actuators will not be able to deliver sufficient power due to a fixed (either fracture or breakdown-limited) energy density and reduced operating frequencies. The specific cutoff is highly dependent

● = *highest*, ◕ = *high*, ◑ = *moderate*, ◔ = *low*, ○ = *lowest*

Type	Example	Efficiency	Toughness	Bandwidth[1]	Max. ε	Max. σ	Density
Bulk piezo.	PZT-5H[2]	◔	◔	●	○	◕	●
Single crystal	PZN-PT[3]	◔	○	●	◔	◑	●
SMA	Nitinol[4]	○	◑	◔	◑	●	●
IPMC	Nafion[5]	◔	◑	◔	●	◔	◑
EAP	DE[6]	◔	◑	◑	●	◔	◔
Electromag.	brushless[7]	◑	NA	◑	NA	NA	●

Fig. 7. Qualitative comparison of actuation technologies.

[1]Depends upon structure geometry.

[2]From Piezo Systems: see http://www.piezo.com

[3]Single-crystal piezoelectric ceramics, see Yin et al. (2000)

[4]Shape memory alloy: see http://www.dynalloy.com

[5]From DuPont, see Lee et al. (2005).

[6]Dielectric elastomers, see Pelrine et al. (2001).

[7]For example, 0308 DC micro-motor from Smoovy: see http://www.faulhaber-group.com

on the details of the vehicle design and will not be discussed here. Finally, we do not assume that piezoelectric actuation is the best choice for all functions of a pico air vehicle. As discussed in Section 2.3, we divide actuation between power delivery and control. The previous discussions have focused on maximizing resonant power delivery in order to generate thrust to maintain flight, however the requirements for a control actuator could be rather different than a power actuator, thus a hybrid solution is a potentially viable option. Furthermore, the function of the actuator (i.e. power versus control) will drive power electronics requirements. Section 2.5 discusses power electronics topologies for piezoelectric power actuators.

2.3. Control

The challenges for control for a pico air vehicle are not in planning and navigation, but rather more fundamental topics of stabilization, sensing, and electromechanical design. Flapping-wing robots similar to the one in Figure 1 are designed such that the mean lift vector passes through the center of mass and the periodic drag forces are symmetric on the upstroke and downstroke, thus there are nominally zero body torques during flight. However, fabrication errors and external disturbances can easily excite instabilities in the roll, pitch, or yaw angles which need to be actively suppressed. Figure 8 displays a typical behavior in the absence of any controller or constraints on the body DOFs for a flapping-wing pico air vehicle. It is worth noting that the robot in Figure 8 survived more than 10 such crashes without any damage, which demonstrates the robustness of the materials and components that constitute the robot.

Our control efforts to date have concentrated on (a) development of the thoracic mechanics to enable modulation of wing trajectories and hence body torques, (b) exploration of appropriate sensor technologies, and (c) methodologies for controller synthesis and related demonstrations. Recent progress in these areas includes the following:

- We have demonstrated the ability to generate lift greater than body mass[16] and perform uncontrolled takeoff experiments such as shown in Figure 8 (Wood, 2008). This provides the baseline aeromechanical design and allows us to quantify the thrust the robot can achieve to help bound payload for sensing and power. For example, we have recently measured thrust-to-weight as high as 3.75-to-1 for a 56 mg flapping-wing robot (Pérez-Arancibia et al., 2011b).
- The original designs presented by Wood (2008) only had the ability to control thrust and one body torque (i.e. pitch torques). We have demonstrated the ability to generate bilateral asymmetry in stroke amplitude using multiple thoracic mechanics configurations (Finio et al., 2009b,a). This involves a morphological separation of power and control actuation similar to the role of the 'indirect' and 'direct' flight muscles in the thoracic mechanics of Dipteran insects (Finio and Wood, 2010).
- Similarly, we have performed experiments with stroke plane deviation as an alternative method for torque generation (Finio et al., 2010).
- Beyond modulating the wing trajectory, we have performed torque measurement experiments which verify that there is a one-to-one relationship between dorsoventral mean stroke angle bias and the resulting pitch torque (Finio et al., 2011).
- Through collaborations with Centeye, Inc.,[17] insect-inspired optical flow sensors have been integrated onboard a gliding MAV (Wood et al., 2007).
- Work at U.C. Berkeley has prototyped a number of insect-inspired inertial and horizon-detection sensors such as a biomimetic haltere (similar to the Coriolis force sensing structures in Diptera (Nalbach, 1993)) and

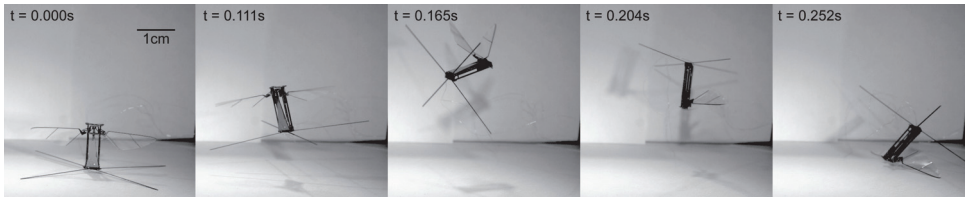

Fig. 8. When driven open-loop, the RoboBee prototypes are very unstable in body rotations and crash shortly after takeoff.

photoreceptive ocelli similar to the horizon detection sensors in insects (Wu et al., 2003).

- Finally, we have implemented an adaptive control scheme to control the mean lift force during flapping (Pérez-Arancibia et al., 2011c) and have demonstrated altitude (Pérez-Arancibia et al., 2011b) and pitch control (Pérez-Arancibia et al., 2011a), with other body DOFs constrained, by modulating stroke amplitude and stroke angle bias respectively.

Our efforts in these areas demonstrate that the pico air vehicle shown in Figure 1 has the ability to generate thrusts greater than vehicle mass and simultaneous wing motion asymmetries to control body moments. This is done in an under-actuated manner, where we retain the simplicity of a single power actuator combined with passively rotating wings (Whitney and Wood, 2010) and supplement with smaller, low-power control actuators to modulate the transmission properties thereby creating the wing motion asymmetries. This is in contrast to previous flapping-wing robotic insects that attempt to actively control both flapping and rotation DOFs in each wing (i.e. four total DOFs (Avadhanula et al., 2002)). The design in Avadhanula et al. (2002) uses two actuators per wing, resulting in a two-input, two-output (i.e. flapping and rotation) dynamical system. Attempting to operate the system at the flapping resonance requires significant attention to design and fabrication of the transmission mechanism to minimize coupling between the two modes (i.e. minimizing the off-diagonal terms in the mapping between actuator inputs and two-DOF wing motions). This is avoided by the use of a passively rotating wing (Wood, 2007), but necessitates the study of alternative thoracic mechanics to generate appropriate body torques. Furthermore, we have demonstrated a methodology for synthesizing controllers based upon experimentally identified models of the robot plant. This is important since fabrication errors can result in performance variations between robots of the same design.

The control efforts discussed above are primarily focused on the standard feedback control strategy in which a disturbance is detected by a proprioceptive sensor, a computer chooses a compensatory action according to some control law, and the action is then implemented by a system of amplifiers and electromechanical structures. We refer to devices which perform such complex tasks without the intervention of electrical circuits (i.e. analog or digital computers) as examples of 'mechanical intelligence'. There are many everyday examples including windshield wipers, whippletrees, and automobile differentials. In these examples, feedback control is performed as a consequence of the mechanical design. For example, automobile differentials automatically distribute equal torques to the wheels regardless of differences in wheel velocities. We have applied this concept to the passive regulation of wing motions by a modified version of the flexure-based transmission called PARITy: 'Passive Aeromechanical Regulation of Unbalanced Torques' (Sreetharan and Wood, 2010). The PARITy design equally distributes torques to the wings in response to perturbations, due to either external disturbances or fabrication errors, without the need for sensors or computation. This allows an active controller to operate on a much longer time scale since short time scale perturbations are eliminated, thereby reducing the required sensor bandwidth and computation power.

2.4. Fabrication

The integrated circuit revolution of the 1950s and 1960s now enables the majority of the consumer electronics that are enjoyed daily. As these techniques evolved in the 1980s to include electromechanical components, an even greater space of applications emerged including sensors, optics, and even actuation (Petersen, 1982). Microrobots have been made using MEMS surface and bulk micromachining techniques (Yeh et al., 1996; Donald et al., 2006). However, there are many drawbacks to using integrated circuit (IC) and MEMS technologies to create a pico air vehicle. First is the dramatic difference between the material properties of silicon and insect tissue: the former being rigid and brittle while the latter exhibits a large range of material properties, is generally quite resilient, and is approximately the density of water. Second, although the suite of techniques for high-resolution machining is an appealing aspect of MEMS processes, the resulting structures are typically '2.5D', with high-aspect-ratio components being extremely challenging in terms of machining or requiring hinged structures (Pister et al., 1992). Finally, although MEMS foundries exist (e.g. the Multi-User MEMS Process, MUMPS[18] and Sandia's SUMMiT[19]), cost and turnaround time are generally prohibitive to rapid prototyping. With the advent of mesoscopic manufacturing methods (Wood et al., 2008; Whitney et al., 2011), we have demonstrated key components of the flight apparatus of robotic insects (Wood et al., 2005; Wood, 2007) and recently the first demonstration of a 60 mg

flapping-wing device which can produce thrust greater than its body weight (Wood, 2008) has proven the feasibility of creating insect-scale flying robots using these techniques.

Mesoscopic manufacturing based on lamination and folding is depicted in Figure 9. This consists of three primary steps. First, the constituent materials, typically thin sheets of polymers, metals, ceramics, or composites, are laser micromachined to the desired planar geometries. These layers are then aligned and laminated using thermoset sheet adhesives and a heated press. Next, the quasi-planar devices are released using a final laser machining step. Finally, the devices are folded into their final configuration. In the case of the spherical five-bar shown in the bottom of Figure 9, tabs and slots are integrated to assist with alignment during folding, although there are other methods to ensure precision in this final step including fixturing, surface tension, differential thermal expansion, pop-up book techniques (Whitney et al., 2011), and even embedded actuation (Paik et al., 2010). This process enables the development of articulated components with any number of DOFs, layered actuators such as the piezoelectric bending actuators described in Section 2.2, and integrated electronics, all with feature sizes ranging from micrometers to centimeters. The concept of folding as an assembly process has been further developed into a larger space of applications for 'Programmable Matter' using robotic origami to produce arbitrary shapes and functional structures (Hawkes et al., 2010). Once each of the components is assembled, Figure 10 shows the integration of a pico air vehicle consisting of an airframe, actuator, transmission, and wings.

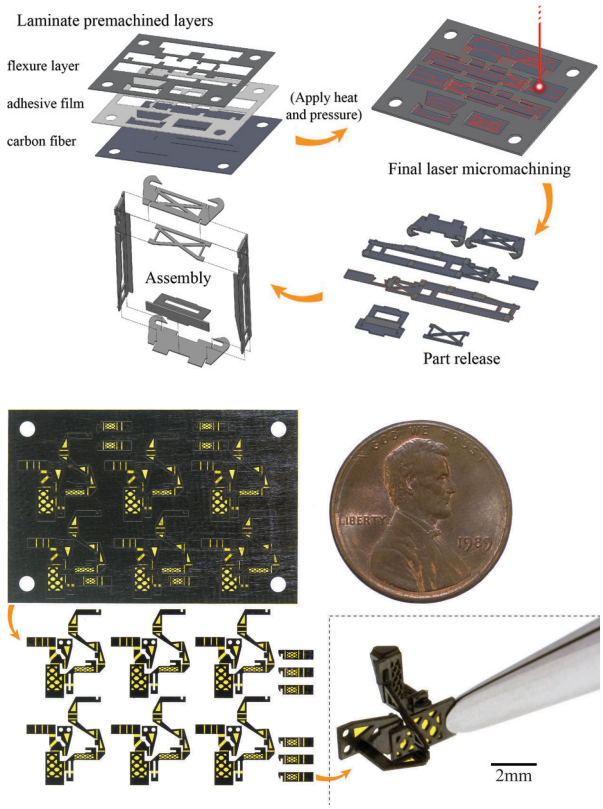

Fig. 9. Example of the process flow for articulated microstructures. The process consists of three primary steps as illustrated in the top figure: machining and lamination of individual layers, release, and assembly. Assembly typically relies on a combination of mating features and folding. In the bottom example, this process creates six spherical five-bar linkages that are folded into the final configuration (inset).

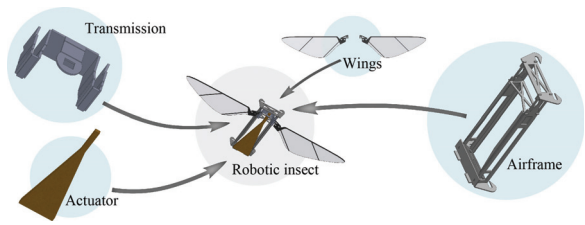

Fig. 10. Post-fabrication, the primary aeromechanics components are integrated to complete the robotic insect. This is typically accomplished manually using mating features machined during fabrication.

2.5. Power

The power source for a pico air vehicle is the most significant limiter to flight time (Karpelson et al., 2010). Options for power storage include electrochemical (i.e. batteries and fuel cells (Tsuchiya et al., 2011)), electrostatic (i.e. capacitors and supercapacitors), and mechanical (i.e. elastic strain energy).[20] As with all components, practicality is a fundamental consideration. Existing batteries have poor energy storage (approximately 500 J/g based on existing small-scale lithium batteries from Fullriver[21]) compared with fuels such as gasoline which can be two orders of magnitude greater. But energy density alone is not sufficient to describe the effectiveness of a candidate power source. Conversion efficiency, storage/packaging, and operating conditions should also be considered. For example, consider a scaled version of an internal combustion engine. Not only are the rotating and reciprocating components challenging to scale down, liquid or gaseous fuel storage becomes problematic at smaller scales since an increasing surface-area-to-volume ratio requires more material to be expended on packaging.

There are sub-gram batteries which are commercially available.[22] While the lower end of this range (approximately 200 mg) could be acceptable for a pico air vehicle, smaller batteries are feasible, although rare or non-existent as commercial products. Since the electrochemical reactions are scale-independent (at least for the scales considered here), creating smaller batteries becomes an exercise in fabrication and packaging. For example, it is possible to dice and repackage lithium-polymer batteries in an inert atmosphere.

Power distribution efficiency is also a fundamental concern. Assuming the source will have a voltage of approximately 3.7 V, and using the piezoelectric actuator

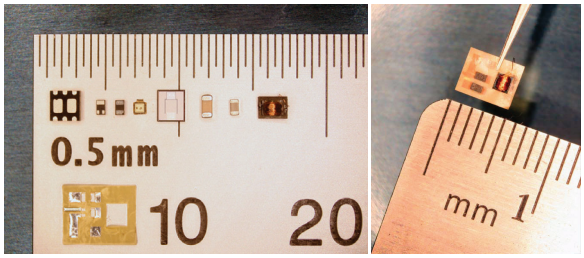

Fig. 11. Components (left) and a complete tapped-inductor-based 20 milligram boost conversion circuit (right).

dimensions from Wood et al. (2005), the power distribution circuits for a pico air vehicle will require a boost conversion stage with a step-up ratio in the range of 50–100 (Steltz et al., 2006). Options for boost conversion include piezoelectric transformers, charge pump ladder circuits, and electromagnetic transformers. Once the source voltage is boosted to the proper level, the actuator drive signal is generated. Considering the low electromechanical coupling coefficients for many piezoelectric materials, it is essential to recover remaining charge from one half cycle of the harmonic oscillation of the thorax and use for the next half cycle. Charge recovery circuits for bimorph actuators have been developed (Campolo et al., 2003) and a custom integrated circuit which generates the periodic drive signal and coordinates charge recovery has been created and demonstrated for a flapping-wing robot (Karpelson et al., 2011). Therefore, the power source is the key remaining technology required to bring the pico air vehicle in Figure 1 to power autonomy.

3. Next steps

The progress on pico air vehicles reported in this article is the tip of the iceberg. The next steps include the following:

- **Power source:** Characterization of batteries and other viable power sources (including supercapacitors and micro fuel cells) under appropriate loading conditions.
- **Integration:** The best demonstration for any core technology involves integration onto a flight-worthy robot.
  - *On-board sensors*: Continued collaboration with manufacturers of optical flow sensors (Centeye, Inc.), aiming to demonstrate a flight-worthy sensor and use in altitude control experiments.
  - *On-board power electronics:* Integrating the components from Figure 11 into the airframe utilizing the layered manufacturing technique described in Section 2.4.
- **Accelerator-based computation:** The RoboBees project is exploring compute architectures which employ highly specialized integrated circuits to perform a single task (such as control or sensor processing) extremely efficiently (Lyons et al., 2010).
- **System-level design and optimization:** Finally, while much attention has been paid to each component, there have been few efforts for system-level optimization for vehicles of this scale. The work of Karpelson et al. (2010) suggests the most promising areas to focus design efforts and how improvements to the performance of any sub-system will contribute to increased flight time.

Notes

1. Section 220 of the National Defense Authorization Act for Fiscal Year 2001 states that, 'It shall be the goal of the Armed Forces to achieve the fielding of unmanned, remotely controlled technology such that... by 2010, one-third of the aircraft in the operational deep strike force aircraft fleet are unmanned' (106th Congress, 2000).
2. See http://www.defense.gov/releases/release.aspx?releaseid=1538
3. See http://www.fbo.gov/index?s=opportunity&mode=form&id=e88cb2b0a71e6487c60283c05de48ceb&tab=core&_cview=1
4. See http://www.avinc.com/nano/
5. See http://www.atl.lmco.com/papers/1448.pdf
6. See http://www.draper.com/Documents/explorations_summer2010.pdf
7. See http://www.wowwee.com/en/products/toys/flight/flytech
8. See http://robobees.seas.harvard.edu
9. For example, Microlution 5100: see http://microlution-inc.com/products/5100.php
10. See http://www.teslamotors.com/roadster/specs
11. SBL02-06H1 from Namiki: see http://www.namiki.net/product/dcmotor/pdf/sbl02-06ssd04_01_e.pdf
12. Note that this does not include drive circuitry, which is also exacerbated at small scales.
13. 'Squiggle' motors: see http://www.newscaletech.com/squiggle_overview.html
14. For a discussion of scaling issues for microrobots, see Trimmer (1989).
15. The resonant frequency is $\omega_0 = \sqrt{k_{eq}/m_{eq}}$. In the case of a linear spring, $k_{eq} \propto L$ and $m_{eq} \propto L^3$. In the case of a clamped–free cantilever beam, $k_{eq} \propto L^3$ and $m_{eq} \propto L^5$. In both cases, $\omega_0 \propto L^{-1}$.
16. Body mass here refers to the total mass of the vehicle. In our test cases to date, this is relaxed by the use of power tethers (i.e. externally supplied power), but for a fully autonomous case, this would include the total mass of the entire system.
17. See http://www.centeye.com
18. See http://www.memscapinc.com
19. See http://www.mems.sandia.gov/tech-info/summit-v.html
20. Note that this only refers to storage, not transduction or harvesting.
21. See http://www.fullriver.com/
22. See note 21.

Funding

This work was partially supported by the National Science Foundation (award number CCF-0926148), the Army Research Laboratory (award number W911NF-08-2-0004), the Office of

Naval Research (award number N00014-08-1-0919), the Air Force Office of Scientific Research (award number FA9550-09-1-0156), and the Wyss Institute for Biologically Inspired Engineering. Any opinions, findings, and conclusions or recommendations expressed in this material are those of the authors and do not necessarily reflect the views of the National Science Foundation.

References

106th Congress (2000) National Defense Authorization Act, Fiscal Year 2001. Public Law 106-398, 106th Congress.

Avro Canada (2010) Avro Canada VZ-9AV Avrocar. http://www.nationalmuseum.af.mil/factsheets/factsheet.asp?id=10856.

Avadhanula S, Wood R, Campolo D and Fearing R (2002) Dynamically tuned design of the MFI thorax. In *IEEE International Conference on Robotics and Automation*, Washington, DC.

Bellew C, Hollar S and Pister K (2003) An SOI process for fabrication of solar cells, transistors, and electrostatic actuators. In *The 12thth International Conference on Solid State Sensors, Actuators and Microsystems*, pp. 1075–1079.

Bergou A, Xu S and Wang Z (2007) Passive wing pitch reversal in insect flight. *Journal of Fluid Mechanics* 591: 321–337.

Brooks R and Flynn A (1989) Fast, cheap and out of control: A robot invasion of the Solar System. *Journal of the British Interplanetary Society* 42: 478–485.

Campolo D, Sitti M and Fearing R (2003) Efficient charge recovery method for driving piezoelectric actuators in low power applications. *IEEE Transactions on Ultrasonics, Ferroelectrics and Frequency Control* 50: 237–244.

Caprari G, Estier T and Siegwart R (2002) Fascination of down scaling - alice the sugar cube robot. *Journal of Micromechatronics* 1: 177–189.

Combes S and Daniel T (2003a) Flexural stiffness in insect wings II. Spacial distribution and dynamic wing bending. *Journal of Experimental Biology* 206: 2989–2997.

Combes S and Daniel T (2003b) Into thin air: Contributions of aerodynamic and inertial-elastic forces to wing bending in the hawkmoth *Manduca sexta*. *Journal of Experimental Biology* 206: 2999–3006.

Cox A, Monopoli D, Cveticanin D, Goldfarb M and Garcia E (2002) The development of elastodynamic components for piezoelectrically actuated flapping micro-air vehicles. *Journal of Intelligent Material Systems and Structures* 13: 611–615.

Dickinson M, Lehmann F-O and Sane S (1999) Wing rotation and the aerodynamic basis of insect flight. *Science* 284: 1954–1960.

Donald B, Levey C, McGray C, Paprotny I and Rus D (2006) An untethered, electrostatic, globally controllable MEMS microrobot. *Journal of Microelectrical Mechanical Systems* 15: 1–15.

Dudley R (1999) *The Biomechanics of Insect Flight: Form, Function and Evolution*. Princeton, NJ: Princeton University Press.

Ellington C, van der Berg C, Willmott A and Thomas A (1996) Leading-edge vortices in insect flight. *Nature* 384: 626–630.

Ennos A (1988a) The importance of torsion in the design of insect wings. *Journal of Experimental Biology* 140: 137–160.

Ennos A (1988b) The inertial cause of wing rotation in Diptera. *Journal of Experimental Biology* 140: 161–169.

Fearing R, Avadhanula S, Campolo D, Sitti M, Yan J and Wood R (2002) A micromechanical flying insect thorax. In *Neurotechnology for Biomimetic Robots*. Cambridge, MA: The MIT Press, pp. 469–480.

Fearing R, Chang K, Dickinson M, Pick D, Sitti M and Yan J (2000). Wing transmission for a micromechanical flying insect. In *IEEE International Conference on Robotics and Automation*.

Finio B, Eum B, Oland C and Wood, R. (2009a). Asymmetric flapping for a robotic fly using a hybrid power-control actuator. In *IEEE International Conference on Robotics and Automation*, St. Louis, MO.

Finio B, Galloway K and Wood R (2011) An ultra-high precision, high bandwidth torque sensor for microrobotics applications. In *IEEE/RSJ International Conference on Intelligent Robots and Systems*, San Francisco, CA.

Finio B, Shang J and Wood R (2009b) Body torque modulation for a microrobotic fly. In *IEEE International Conference on Robotics and Automation*, Kobe, Japan, pp. 3449–3456.

Finio B, Whitney J and Wood R (2010) Stroke plane deviation for a microrobotic fly. In *IEEE/RSJ International Conference on Intelligent Robots and Systems*, Taipei, Taiwan.

Finio B and Wood R (2010) Distributed power and control actuation in the thoracic mechanics of a robotic insect. *Bioinspiration and Biomimetics* 5: 045006.

Hawkes E, An B, Benbernou N, Tanaka H, Kim S, Demaine E, et al. (2010) Programmable matter by folding. *Proceedings of the National Academy of Sciences of the USA* 107: 12441–12445.

Karpelson M, Wei G-Y and Wood R (2008) A review of actuation and power electronics options for flapping-wing robotic insects. In *IEEE International Conference on Robotics and Automation*, Pasadena, CA.

Karpelson M, Whitney J, Wei G-Y and Wood R (2010) Energetics of flapping-wing robotic insects: towards autonomous hovering flight. In *IEEE/RSJ International Conference on Intelligent Robots and Systems*, Taipei, Taiwan.

Karpelson M, Wood R and Wei G-Y (2011) Low power control ic for efficient high-voltage piezoelectric driving in a flying robotic insect. In *Symposium on VLSI Circuits*, Kyoto, Japan.

Keennon M and Grasmeyer J (2003) Development of the Black Widow and Microbat MAVs and a vision of the future of MAV design. In *AIAA/ICAS International Air and Space Symposium and Exposition: The Next 100 Years*, Dayton, OH.

Lee S, Park H and Kim K (2005) Equivalent modeling for ionic polymer metal composite actuators based on beam theories. *Smart Materials and Structures* 14: 1363–1368.

Lentink D, Jongerius S and Bradshaw N (2009) The scalable design of flapping micro-air vehicles inspired by insect flight. In *Flying Insects and Robots*. New York: Springer Verlag, pp. 185–205.

Lyons M, Hempstead M, Wei G-Y and Brooks D (2010) The accelerator store framework for high-performance, low-power accelerator-based systems. *IEEE Computer Architecture Letters* 9: 53–56.

Mittal R and Iaccarino G (2005) Immersed boundary methods. *Annual Review of Fluid Mechanics* 37: 239–261.

Nalbach G (1993) The halteres of the blowfly *Calliphora* I. Kinematics and dynamics. *Journal of Comparative Physiology A* 173: 293–300.

Newnham R, Dogan A, Xu Q, Onitsuka K, Tressler J and Yoshikawa S (1993) Flextensional "moonie" actuators. In *Proceedings IEEE Ultrasonics Symposium*, Baltimore, MD, volume 1, pp. 509–513.

Paik J, Hawkes E and Wood R (2010) A novel low-profile shape memory alloy torsional actuator. *Journal of Smart Materials and Structures* 19: 125014.

Pelrine R, Sommer-Larsen P, Kornbluh R, Heydt R, Kofod G, Pei Q, et al. (2001) Applications of dielectric elastomer actuators. In *Proceedings of the International Society for Optical Engineering* 4329: 335–349.

Pérez-Arancibia N, Chirarattananon P, Finio B and Wood R (2011a) Pitch-angle feedback control for a bio-inspired flapping-wing microrobot. In *IEEE International Conference on Robotics and Biomimetics*, Phuket Island, Thailand.

Pérez-Arancibia N, Ma K, Galloway K, Greenberg J and Wood R (2011b). First controlled vertical flight of a biologically inspired microrobot. *Bioinspiration and Biomimetics* 6: 036009.

Pérez-Arancibia N, Whitney J and Wood R (2011c) Lift force control of a flapping-wing microrobot. In *American Control Conference*, San Francisco, CA.

Petersen K (1982) Silicon as a mechanical material. *Proceedings of the IEEE* 70: 420–457.

Pister K, Judy M, Burgett S and Fearing R (1992) Microfabricated hinges. *Journal of Sensors and Actuators A: Physical* 33: 249–256.

Shang J, Combes S, Finio B and Wood R (2009) Artificial insect wings of diverse morphology for flapping-wing mavs. *Bioinspiration and Biomimetics* 4: 036002.

Shen S, Michael N and Kumar V (2011) Autonomous multi-floor indoor navigation with a computationally constrained MAV. In *IEEE International Conference on Robotics and Automation*, Shanghai, China.

Sreetharan P and Wood R (2010) Passive aerodynamic drag balancing in a flapping wing microrobotic insect. *Journal of Mechanical Design* 132: 051006–051016.

Steltz E and Fearing R (2007) Dynamometer power output measurements of piezoelectric actuators. In *IEEE/RSJ International Conference on Intelligent Robots and Systems*, San Diego, CA.

Steltz E, Seeman M, Avadhanula S and Fearing R (2006) Power electronics design choice for piezoelectric microrobots. In *IEEE/RSJ International Conference on Intelligent Robots and Systems*, Beijing, China.

Stirling T and Floreano D (2010) Energy-time efficiency in aerial swarm deployment. In *Proceedings of the 10th International Symposium on Distributed Autonomous Robotics Systems.*

Tanaka H, Hoshino K, Matsumoto K and Shimoyama I (2005) Flight dynamics of a butterfly-type ornithopter. In *IEEE/RSJ International Conference on Intelligent Robots and Systems*, Edmonton, Alberta, Canada.

Tanaka H, Whitney J and Wood R (2011) Effect of flexural and torsional wing flexibility on lift generation in hoverfly flight. *Journal of Integrative and Comparative Biology* 51: 142–150.

Tanaka H and Wood R (2010) Fabrication of corrugated artificial insect wings using laser micromachined molds. *Journal of Micromechanics and Microengineering* 20(7): 075008.

Tang W, Nguyen T-C, Judy M and Howe R (1990) Electrostatic-comb drive of lateral polysilicon resonators. *Journal of Sensors and Actuators A: Physical* 21: 328–331.

Trimmer W (1989) Microrobots and micromechanical systems. *Journal of Sensors and Actuators* 19: 267–287.

Tsuchiya M, Lai B and Ramanathan S (2011) Scalable nanostructured membranes for solid oxide fuel cells. *Nature Nanotechnology* 6: 282–286.

Vincent J and West U (2004) Design and mechanical properties of insect cuticle. *Arthropod Structure and Development* 33: 187–199.

Whitney J, Sreetharan P, Ma K and Wood R (2011) Pop-up book MEMS. *Journal of Micromechanics and Microengineerings* 6: 036009.

Whitney J and Wood R (2010) Aeromechanics of passive rotation in flapping flight. *Journal of Fluid Mechanics* 660: 197–220.

Wood R (2007) Design, fabrication, and analysis, of a 3DOF, 3cm flapping-wing MAV. In *IEEE/RSJ International Conference on Intelligent Robots and Systems*, San Diego, CA.

Wood R (2008) The first flight of a biologically-inspired at-scale robotic insect. *IEEE Transactions on Robotics* 24: 341–347.

Wood R, Avadhanula S, Sahai R, Steltz E and Fearing R (2008) Microrobot design using fiber reinforced composites. *Journal of Mechanical Design* 130(5): .

Wood R, Avadhanula S, Steltz E, Seeman M, Entwistle J, Bachrach A, et al. (2007) An autonomous palm-sized gliding micro air vehicle. *Robotics and Automation Magazine* 14: 82–91: 052304.

Wood R, Cho K-J and Hoffman K (2009) A novel multi-axis force sensor for microrobotics applications. *Journal of Smart Materials and Structures* 18: 125002.

Wood R, Steltz E and Fearing R (2005) Optimal energy density piezoelectric bending actuators. *Journal of Sensors and Actuators A: Physical* 119: 476–488.

Wu W, Schenato L, Wood R and Fearing R (2003) Biomimetic sensor suite for flight control of a micromechanical flying insect: Design and experimental results. In *IEEE International Conference on Robotics and Automation*, Taipei, Taiwan.

Yeh R, Kruglick E and Pister K (1996) Surface-micromachined components for articulated microrobots. *Journal of Microelectrical Mechanical Systems* 5: 10–17.

Yin J, Jiang B and Cao W (2000) Elastic, piezoelectric, and dielectric properties of $0.995Pb(Zn_{1/3}Nb_{2/3})O_3 - 0.45PbTiO_3$ single crystal with designed multidomains. *IEEE Transactions on Ultrasonics, Ferroelectrics, and Frequency Control* 47: 285–291.